

# A Landau Theory for Pair Density Modulation in Fe(Te,Se) flakes.

Po-Jui Chen<sup>1</sup> and Piers Coleman<sup>1, 2, \*</sup>

<sup>1</sup>*Department of Physics and Astronomy, Rutgers University, Piscataway, New Jersey 08854, USA*

<sup>2</sup>*Department of Physics, Royal Holloway University of London, Egham, Surrey TW20 0EX, United Kingdom*

(Dated: December 11, 2025)

Motivated by recent scanning tunneling microscopy (STM) experiments reporting a pair-density modulation (PDM) in  $\text{FeTe}_{0.55}\text{Se}_{0.45}$ , we develop a Landau theory to elucidate the physical origin of this phenomenon. We analyze the PDM in terms of the screw symmetry of the single layer, interpreting it as a hybridized state of two order parameters of opposite glide and screw parity. Discussing the absence of PDM in the bulk where both glide and screw symmetry are present, we argue that the absence of glide symmetry on the surface allows nematic order to selectively stabilize the PDM in thin flakes. Finally, we discuss the symmetry constraints on the microscopic pairing mechanism, pointing out the opposite glide and screw parities of the order parameters favor a site, rather than a bond-based paring mechanism. This suggests that pairing in iron-based superconductors may be *local* to the iron atoms, possibly driven by Hunds coupling.

*Introduction.* Iron-based superconductors [1–6] provide a fertile platform for exploring a wide variety of correlated electronic phases. Numerous experiments point towards an unconventional origin for the superconductivity in these materials [5, 7, 8]. A new kind of modulated superconducting state was discovered in recent scanning tunneling microscopy (STM) experiments[9–12] on ultra-thin flakes of  $\text{FeTe}_{0.55}\text{Se}_{0.45}$ , which reveal[11] that the superconducting gap differs by up to 40% on the two iron sublattices, forming a “pair density modulated state” (PDM). Two sequential superconducting transitions are observed on cooling[11]: first, uniform superconductivity develops at 11K, then a second transition into the PDM state occurs at 9K (see Fig.1 (a)). In the PDM, the gap, defined by one half the peak-to-peak separation in the density of states, becomes different at the two iron sites, A and B, in the unit cell. The gap modulation  $(\Delta_A - \Delta_B)/(\Delta_A + \Delta_B) = \pm f$  is  $f = 20\%$  in the sample principally studied in experiments, but was observed to rise to  $f = 40\%$  in the thinnest flakes, while entirely vanishing in the thickest samples. Moreover, the modulated gap structure is also accompanied by a nematic order, forming domains in which the square iron plaquettes undergo a rhombohedral compression(see Fig. 2(c)) or expansion of about 1% along their diagonals.

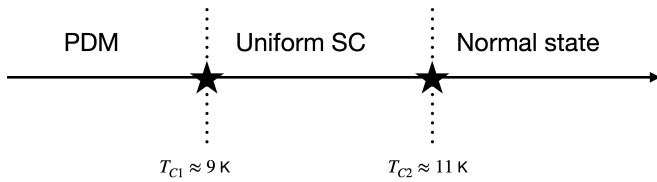


FIG. 1. Schematic illustration of the two-step phase transition. The ground state evolves from PDM state into a uniform superconducting order and then into a normal state. The two critical temperatures are  $T_{c1} \approx 9\text{K}$  and  $T_{c2} \approx 11\text{K}$  [11].

The PDM is particularly intriguing because it resembles a pair-density-wave (PDW) state[7] in which the superconducting order parameter also develops spatial modulation. However, unlike the PDW, the PDM does not break translational symmetry: in this sense it reminds us of its magnetic counterpart, the altermagnet[13], for both share the common feature that they preserve lattice translational symmetry, because of a non-symmorphic crystal structure with two magnetic atoms per unit cell. A second distinct feature of the PDM is that it develops spontaneously, in the absence of a pre-existing broken symmetry in the normal state, such as a Zeeman split Fermi surface [14, 15] or charge density-wave order[16, 17] that often accompany PDWs.

In bulk  $\text{FeSe}_{1-x}\text{Te}_x$  the iron atoms form stacked square lattice layers with the chalcogenide Se or Te atoms alternately located above or below neighboring iron plaquettes. This gives rise to a non-symmorphic structure described by space group P4/nmm(No.129)[18, 19] with two iron atoms per unit cell. The structure is invariant under a glide-mirror ( $\tilde{M}_z$ ) and a screw operation ( $\tilde{C}_4$ ):

$$\tilde{M}_z = M_z T_{(1/2,1/2)}, \quad \tilde{C}_4 = R_{\pi/2} T_{(1/2,1/2)} \quad (1)$$

corresponding to half-lattice translation  $T_{(1/2,1/2)}$  followed by either a reflection in the  $xy$  plane ( $M_z$ ) or a  $\pi/2$  rotation about the z-axis ( $R_{\pi/2}$ ) (see Fig.2(a)). However, in a thin flake, the chalcogenide atoms lie at different distances above and below the iron-plane(see Fig. 2), removing the mirror symmetry[11], leaving just the screw symmetry to protect the equivalence of the two iron atoms, and it is this symmetry that is broken by the PDM order. Many experimental observations have reported the existence of nematic order  $\Phi$  [8, 20] in  $\text{Fe}(\text{Te},\text{Se})$  or monolayer  $\text{FeSe}$ , which also breaks the screw symmetry which must therefore be considered as an important element in the development of the PDM.

In a recent paper, Papaj, Kong, Nadj-Perge and Lee (PKPL)[21] propose a BCS description of the PDM state based on the loss of the glide-mirror symmetry. In their model, the development of a hybrid order parameter  $s_{\pm} +$

\* Second.Author@institution.edu

$d$  between an extended s- and d-wave superconducting phase removes the equivalence between the two lattice sites and giving rise to a modulated gap structure. While the PKPL theory provides an illustration of a PDM, the role of the symmetries are hidden within the structure of the internal tight-binding model and the assumed BCS couplings. In particular, the screw symmetry of the flakes does not play an explicit role in their theory.

Here, we develop a complementary description of the PDM based on Landau theory: our philosophy is to use the experimental properties of the PDM to gain insight into the microscopic physics. Landau theory allows us to observe the role of the order-parameter symmetry, and its interplay with nematic order; in particular, the screw symmetry of the flakes plays a central role in our theory. Here we are particularly interested in understanding why the PDM is present in thin flake samples, yet absent in the bulk. Moreover, our approach allows us to consider the constraints on the underlying pairing mechanism that are imposed by the properties of the PDM.

On rather general grounds, screw symmetry must play a central role in the development of the PDM, for the order parameters which mix to produce the PDM must form representations of the screw symmetry, with a well-defined eigenvalue under the screw operation. Assuming that time-reversal symmetry is unbroken, we argue that the PDM phase arises from a hybridization of two order parameters of opposite parity under the screw symmetry that is specific to the thin-flake geometry. Generically, two different order parameters are separated by a first order phase transition. We argue that the coupling of the two order parameters to nematicity is only permitted at the surface, and it is this coupling that creates the hybridized PDM in the thin flakes. This places some rather interesting constraints on the pairing that we raise in the conclusion.

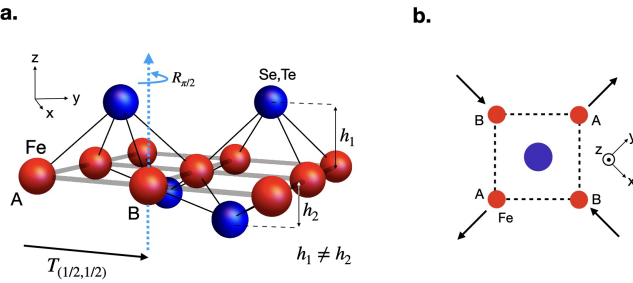


FIG. 2. **a.** Structure of single-layer Fe(Te,Se) showing the different distance of the upper and lower chalcogenide atoms from the iron plane. **b.** atomic displacements associated with nematic order. These displacements change sign under a  $\pi$  rotation.

Under the screw rotation  $\tilde{C}_4$ , the superconducting order parameter generally transforms as  $\tilde{C}_4^{-1}\Delta\tilde{C}_4 = e^{im\pi/2}\Delta$ , where  $m$  is the angular momentum quantum number. In our discussion, we focus on the time-reversal-symmetric cases with  $m = 0, 2$ , for which  $\tilde{C}_4^{-1}\Delta_{\pm}\tilde{C}_4 =$

$\pm\Delta_{\pm}$ . The transformation properties of  $\Delta_+$ ,  $\Delta_-$  and  $\Phi$  are listed in Table I.

Order Parameter	$\Phi$	$\Delta_+$	$\Delta_-$
$\tilde{C}_4$ eigenvalues	-1	+1	-1

TABLE I. Symmetry of the three order parameters under fourfold screw operation  $\tilde{C}_4$ .

*Landau free energy.* To describe the PDM state, we develop the Landau free energy which involves three order parameters: nematic order  $\Phi$  and two superconducting orders with different parity  $\Delta_+$ ,  $\Delta_-$ ,

$$F = F_{\Delta} + F_{\Delta\Phi}, \quad (2)$$

where

$$\begin{aligned} F_{\Delta} &= a[(T - T_c^+)^2 + (T - T_c^-)^2] \\ &\quad + \frac{1}{2}(u_+\Delta_+^4 + u_-\Delta_-^4 + 2u_{\pm}\Delta_+^2\Delta_-^2), \quad (3) \\ F_{\Delta\Phi} &= \alpha\Phi^2 + \lambda\Phi\Delta_+\Delta_-. \end{aligned}$$

Here  $F_{\Delta}$  is the superconducting part of the free energy, while  $F_{\Delta\Phi}$  describes the nematic order and its coupling to the superconductivity.  $T_c^+$  and  $T_c^-$  characterize the intrinsic superconducting transition temperatures of the two order parameters, tuned by an external field  $g$ , so that  $T_c^{\pm} = T_0 \pm g$  where  $g = 0$  corresponds to the point where the transition temperatures are equal.  $a > 0$  and  $u_-$ ,  $u_{\pm}$  and  $u_+$  define the repulsion between the two order parameters. Quartic terms that contain an odd power of  $\Delta_+$  or  $\Delta_-$  are excluded, since these are not invariant under the screw symmetry. Finally note that we assume that the two order parameters are phase-locked with a single overall phase that can be factored out of the free energy.

The second term  $F_{\Delta\Phi}$  describes the nematic order and its coupling to the superconductivity.  $\text{FeTe}_{0.55}\text{Se}_{0.45}$  lies in close proximity to a nematic quantum critical point[20, 22], but does not actually exhibit long-range nematic order, permitting us to approximate the nematic component by a simple quadratic function  $\alpha\Phi^2$ , where the  $\alpha > 0$  denotes the distance from the nematic critical point. The minimal symmetry-allowed coupling  $\Phi\Delta_+\Delta_-$  is the only term permitted by the screw symmetry, given  $\Phi$  has odd-parity under screw rotations.

Our Landau theory highlights the importance of nematic fluctuations. Generically, the phase boundary between the even and odd-parity phases, depends on the strength  $u_{\pm}$  of the repulsion between the order parameters (a detailed derivation is provided in the supplementary materials): if  $u_{\pm} > U_c$  exceeds the critical value

$$U_c = \sqrt{u_+u_-} \quad (4)$$

the transition between the two phases is first order as shown in Fig.3a, but if  $u_{\pm} < U_c$  is less than this value, a hybridized co-existence region opens up within the phase

diagram, as shown in Fig. 3b. Now if we “integrate out” the nematic degree of freedom, rewriting

$$F_{\Delta\Phi} \rightarrow \alpha \left( \Phi + \frac{\lambda}{2\alpha} \Delta_+ \Delta_- \right)^2$$

$$u_{\pm} \rightarrow u_{\pm}^* = u_{\pm} - \frac{\lambda^2}{4\alpha}, \quad (5)$$

we see that nematic fluctuations lower the repulsion between the  $\Delta_+$  and  $\Delta_-$  degrees of freedom, while also predicting that nematic order will develop as a secondary order parameter in a PDM with  $\Phi = -\frac{\lambda}{2\alpha} \Delta_+ \Delta_-$  [23].

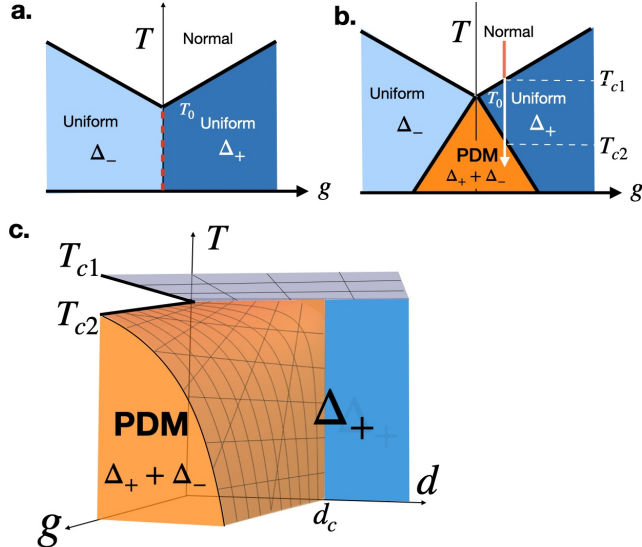


FIG. 3. Phase diagram of the Landau theory showing **a.** when  $u_{\pm} \geq U_c = \sqrt{u_+ u_-}$ , where the co-existence region is absent and **b.** where  $u_{\pm} < U_c = \sqrt{u_+ u_-}$  and a hybridized phase develops. **c.** Representative 3D phase diagram assuming a nematic coupling to the order parameters, exponentially dependent on flake thickness  $d$ , calculated using  $u_{\pm} = 8$ ,  $u_+ = u_- = 2$ ,  $\lambda_0 = 7$ ,  $\alpha = 1$ ,  $\xi = 1$ ,  $T_0 = 1$ .

This suggests a natural explanation for the absence of the PDM in bulk  $\text{FeTe}_{0.55}\text{Se}_{0.45}$  is that the nematic  $\Phi\Delta_-\Delta_+$  is forbidden by the additional symmetries of the bulk. In the bulk, both glide-mirror and inversion symmetries are restored and  $\Phi$  is even parity under both operations, so if  $\Delta_{\pm}$  have *opposite* parities under either symmetry, the nematic coupling will vanish in the bulk. Provided that the system is close enough to the nematic critical point, (small  $\alpha$ ), so that

$$\frac{\lambda^2}{4\alpha} > u_{\pm} - \sqrt{u_+ u_-} > 0, \quad (6)$$

then by (5),  $u_{\pm} > U_c$  in the bulk, but the nematically suppressed value  $u_{\pm}^* < U_c$  in the flakes, promoting PDM order. As the flakes get thicker, glide symmetry will be restored; modeling the dependence of the nematic coupling  $\lambda$  on thickness  $d$  as  $\lambda(d) = \lambda_0 e^{-\frac{d}{\xi}}$ , where  $\xi$  is the symmetry healing length, then using (6) we can identify

an upper-critical flake thickness for the PDM

$$d_c = \frac{\xi}{2} \ln \left[ \frac{\lambda_0^2}{4\alpha(u_{\pm} - \sqrt{u_+ u_-})} \right]. \quad (7)$$

Fig. 3c. shows the associated phase diagram.

*Discussion—* Let us comment on the possible superconducting pairing configurations that can give rise to the pair-density modulated state. One candidate[21] is a bond-based pairing, in which Cooper pairs consist of electrons mainly residing at different lattice sites. Representative bond-based order parameters are extended-s and d-wave

$$\Delta(k) = \begin{cases} \Delta_+(\cos k_x + \cos k_y) & s_{\pm} \\ \Delta_-(\cos k_x - \cos k_y) & d, \end{cases} \quad (8)$$

where the x-and y-axes lie along the *diagonal* of the iron plaquettes[21]. However, in the bulk, these Cooper pair symmetries transform *identically* under inversion or mirror reflection, so a nematic coupling to the order parameters  $\lambda\Phi\Delta_-\Delta_+$  is permitted in both flakes and the bulk. Thus bond-based pairing, though widely used to model the iron-based superconductors[2, 5, 8], does not provide a natural explanation for the absence of PDM in bulk samples (see Table II).

An intriguing alternative is local pairing [24–28], in which pairs form locally at the iron sites. Here, the likely source of pairing is triplet pairing, driven by strong Hunds coupling inside the iron atoms. In this case, the minimal description involves a competition between a uniform (in-phase) and a staggered (out-of-phase) pairing state[24, 29] within the 2-Fe unit cell. These have opposite glide and screw parities, restricting nematic coupling to the flakes where glide symmetry is absent. Representative order parameters take the form

$$\Delta(\vec{x}) = \begin{cases} \vec{\Delta}_+ \cdot \vec{\sigma}(\sigma_2 \lambda_2) & \text{uniform} \\ \vec{\Delta}_- \cdot \vec{\sigma}(\sigma_2 \lambda_2) e^{i\vec{Q} \cdot \vec{x}} & \text{staggered}, \end{cases} \quad (9)$$

where  $\vec{x}$  is the spatial co-ordinate of the iron sites,  $\vec{\Delta}_{+,-}$  are the d-vectors for the uniform and staggered triplet pairing,  $(\lambda_2)_{\alpha\beta} = -(\lambda_2)_{\beta\alpha}$  is the antisymmetric operator acting on  $t_{2g}$  orbital states, e.g.  $\alpha, \beta \in (d_{zx}, d_{zy})$ , while  $\vec{Q} = (2\pi, 0) \equiv (0, 2\pi)$  is the wave-vector for the PDM. We note that the re-establishment of an inversion center between the Fe-atoms in the bulk ensures that globally, the uniform  $\Delta_+$  phase is an even parity singlet, while the bulk staggered  $\Delta_-$  phase is an odd-parity triplet[24].(see Table II).

The local scenario may also provide a clue to the close vicinity of the two critical temperatures, which would originate from the same atomic interactions, and a more natural account of the 40% variation in gap found in the thinnest flakes. If the hybridized order parameter is  $\alpha\Delta_+ + \beta\Delta_-$ , then a gap modulation factor  $(\Delta_A - \Delta_B)/(\Delta_A + \Delta_B) = f = \frac{\beta}{\alpha}$  can easily accommodate the observed 40% ratio  $f = 0.4$ . Indeed, in the bond-based scenario, production of still thinner flakes may even

$(\Delta_+, \Delta_-)$	$\tilde{M}_z$	$P$	Bulk $\Phi\Delta_+\Delta_-$ symmetry allowed?
( $s_{\pm}$ -wave, d-wave)	(1, 1)	(+, +)	✓
(uniform, staggered)	(1, -1)	(+, -)	✗

TABLE II. Bulk glide-mirror  $\tilde{M}_z$  and spatial parity eigenvalues  $P$  for bond-based and local pairing scenarios, showing that a nematic coupling in the bulk is forbidden in a site-based pairing scenario.

drive  $f > 1$  beyond one, meaning that the phase of the gap function has become staggered[24], a situation which would also be detected using a Josephson STM [27].

The mechanism we have presented here may have broader relevance to other correlated superconductors. Indeed, there is already a precedent for a switch between singlet and triplet pairing in the heavy fermion compound CeRh<sub>2</sub>As<sub>2</sub> which has a non-symmorphic crystal structure with an inversion point between layers[30, 31]; in this case, the application of a magnetic field drives the system

through a first order transition from a singlet to a triplet pairing state, thought to exhibit a staggered superconducting order parameter[31, 32]. This suggests an analogous experiment on iron-based superconductors, testing whether a similar parallel-spin paired state is stabilized by high fields perpendicular to the putative d-vector  $\vec{\Delta}_-$ . Finally, it is interesting to speculate whether parity-mixed superconductivity may occur under the application of strain in other non-symmorphic superconductors, such as UTe<sub>2</sub>[33–35].

## ACKNOWLEDGMENTS

The authors would like to thank Phil Brydon, Po-Yao Chang, Indra Gankuyag, Andreas Gleis, Daniel Kaplan, Liam L.H. Lau, Aaditya Panigrahi, and Kaustubh Roy for discussions related to this project. This work was supported by the Office of Basic Energy Sciences, Material Sciences and Engineering Division, U.S. Department of Energy (DOE) under Contract DE-FG02-99ER45790.

---

[1] A. I. Coldea, Electronic Nematic States Tuned by Iso-electronic Substitution in Bulk FeSe<sub>1-x</sub> S<sub>x</sub>, *Frontiers in Physics* **8**, 594500 (2021).

[2] R. M. Fernandes and A. V. Chubukov, Low-energy microscopic models for iron-based superconductors: A review, *Reports on Progress in Physics* **80**, 014503 (2017).

[3] T. Hanaguri, S. Niitaka, K. Kuroki, and H. Takagi, Unconventional  $s$ -Wave Superconductivity in Fe(Se,Te), *Science* **328**, 474 (2010).

[4] A. Chubukov, Pairing Mechanism in Fe-Based Superconductors, *Annual Review of Condensed Matter Physics* **3**, 57 (2012).

[5] I. I. Mazin, D. J. Singh, M. D. Johannes, and M. H. Du, Unconventional Superconductivity with a Sign Reversal in the Order Parameter of LaFeAsO<sub>1-x</sub>F<sub>x</sub>, *Physical Review Letters* **101**, 057003 (2008).

[6] G. R. Stewart, Superconductivity in iron compounds, *Reviews of Modern Physics* **83**, 1589 (2011).

[7] Y. Liu, T. Wei, G. He, Y. Zhang, Z. Wang, and J. Wang, Pair density wave state in a monolayer high-T<sub>c</sub> iron-based superconductor, *Nature* **618**, 934 (2023).

[8] R. M. Fernandes, A. I. Coldea, H. Ding, I. R. Fisher, P. J. Hirschfeld, and G. Kotliar, Iron pnictides and chalcogenides: A new paradigm for superconductivity, *Nature* **601**, 35 (2022).

[9] Y. Zhang, L. Yang, C. Liu, W. Zhang, and Y.-S. Fu, Visualizing uniform lattice-scale pair density wave in single-layer fese/srtio<sub>3</sub> films (2024), [arXiv:2406.05693](https://arxiv.org/abs/2406.05693).

[10] C. Ding, Z. Xu, X. Jiao, Q. Hu, W. Zhao, L. Yang, K. Jiang, J.-F. Jia, L. Wang, J. Hu, and Q.-K. Xue, Sublattice Dichotomy in Monolayer FeSe Superconductor (2024), [arXiv:2406.15239](https://arxiv.org/abs/2406.15239).

[11] L. Kong, M. Papaj, H. Kim, Y. Zhang, E. Baum, H. Li, K. Watanabe, T. Taniguchi, G. Gu, P. A. Lee, and S. Nadj-Perge, Cooper-pair density modulation state in an iron-based superconductor, *Nature* **640**, 55 (2025).

[12] T. Wei, Y. Liu, W. Ren, Z. Liang, Z. Wang, and J. Wang, Observation of Superconducting Pair Density Modulation within Lattice Unit Cell, *Chinese Physics Letters* **42**, 027404 (2025).

[13] C. Song, H. Bai, Z. Zhou, *et al.*, Altermagnets as a new class of functional materials, *Nature Reviews Materials* **10**, 473 (2025).

[14] P. Fulde and R. A. Ferrell, Superconductivity in a Strong Spin-Exchange Field, *Physical Review* **135**, A550 (1964).

[15] A. I. Larkin and Y. N. Ovchinnikov, Nonuniform state of superconductors, *Zh. Eksp. Teor. Fiz.* **47**, 1136 (1964).

[16] Z. Dai, Y.-H. Zhang, T. Senthil, and P. A. Lee, Pair-Density Waves, Charge-Density Waves, and Vortices in High- T<sub>c</sub> Cuprates, *Physical Review B* **97**, 174511 (2018).

[17] Y. Wang, D. F. Agterberg, and A. Chubukov, Interplay between pair- and charge-density-wave orders in under-doped cuprates, *Physical Review B* **91**, 115103 (2015).

[18] M. H. Fischer, F. Loder, and M. Sigrist, Superconductivity and local noncentrosymmetry in crystal lattices, *Physical Review B* **84**, 184533 (2011).

[19] J. Hu, Iron-Based Superconductors as Odd-Parity Superconductors, *Physical Review X* **3**, 031004 (2013).

[20] K. Ishida, Y. Onishi, M. Tsuji, K. Mukasa, M. Qiu, M. Saito, Y. Sugimura, K. Matsuura, Y. Mizukami, K. Hashimoto, and T. Shibauchi, Pure nematic quantum critical point accompanied by a superconducting dome, *Proceedings of the National Academy of Sciences* **119**, e2110501119 (2022).

[21] M. Papaj, L. Kong, S. Nadj-Perge, and P. A. Lee, Pair density modulation from glide symmetry breaking and nematic superconductivity (2025), [arXiv:2506.19903](https://arxiv.org/abs/2506.19903).

[22] H. Zhao, H. Li, L. Dong, B. Xu, J. Schneeloch, R. Zhong, M. Fang, G. Gu, J. Harter, S. D. Wilson, Z. Wang, and I. Zeljkovic, Nematic transition and nanoscale suppression of superconductivity in Fe(Te,Se), *Nature Physics* **17**, 903 (2021).

[23] A. L. Szabó and A. Ramires, Superconductivity-induced improper orders in nonsymmorphic systems, *Physical Review B* **110**, L180503 (2024).

[24] P. W. Anderson, Further consequences of symmetry in heavy-electron superconductors, *Physical Review B* **32**, 499 (1985).

[25] T. Hazra and P. Coleman, Triplet Pairing Mechanisms from Hund's-Kondo Models: Applications to UTe<sub>2</sub> and CeRh<sub>2</sub>As<sub>2</sub>, *Physical Review Letters* **130**, 136002 (2023).

[26] Y. Komijani, E. König, and P. Coleman, Triplet pairing, orbital selectivity, and correlations in iron-based superconductors, *Physical Review B* **112**, 125120 (2025).

[27] P. Coleman, Y. Komijani, and E. J. König, Triplet Resonating Valence Bond State and Superconductivity in Hund's Metals, *Physical Review Letters* **125**, 077001 (2020).

[28] T.-H. Lee, A. Chubukov, H. Miao, and G. Kotliar, Pairing mechanism in Hund's metal superconductors and the universality of the superconducting gap to critical temperature ratio, *Phys. Rev. Lett.* **121**, 187003 (2018).

[29] T. Hotta and K. Ueda, Odd-parity triplet pair induced by hund's rule coupling, *Phys. Rev. Lett.* **92**, 107007 (2004).

[30] S. Khim, J. F. Landaeta, J. Banda, N. Banenor, M. Brando, P. M. R. Brydon, D. Hafner, R. Küchler, R. Cardoso-Gil, U. Stockert, A. P. Mackenzie, D. F. Agterberg, C. Geibel, and E. Hassinger, Field-Induced Transition within the Superconducting State of CeRh<sub>2</sub>As<sub>2</sub>, *Science* **373**, 1012 (2021).

[31] J. F. Landaeta, P. Khanenko, D. C. Cavanagh, C. Geibel, S. Khim, S. Mishra, I. Sheikin, P. M. R. Brydon, D. F. Agterberg, M. Brando, and E. Hassinger, Field-Angle Dependence Reveals Odd-Parity Superconductivity in CeRh<sub>2</sub>As<sub>2</sub>, *Physical Review X* **12**, 031001 (2022).

[32] C. Lee, D. F. Agterberg, and P. M. R. Brydon, Unified Picture of Superconductivity and Magnetism in CeRh<sub>2</sub>As<sub>2</sub>, *Phys. Rev. Lett.* **135**, 026003 (2025).

[33] D. Aoki, J.-P. Brison, J. Flouquet, K. Ishida, G. Knebel, Y. Tokunaga, and Y. Yanase, Unconventional superconductivity in heavy fermion ute<sub>2</sub>, *Journal of the Physical Society of Japan* **88**, 043702 (2019).

[34] S. K. Lewin, C. E. Frank, S. Ran, J. Paglione, and N. P. Butch, A review of UTe<sub>2</sub> at high magnetic fields, *Reports on Progress in Physics* **86**, 114501 (2023).

[35] P. Coleman, A. Panigrahi, and A. Tsvelik, Solvable 3D Kondo Lattice Exhibiting Pair Density Wave, Odd-Frequency Pairing, and Order Fractionalization, *Physical Review Letters* **129**, 177601 (2022).

## Supplementary materials

### Appendix A: Landau theory: Derivation of Phase boundaries

We recall the effective Landau free energy, which only includes superconducting orders

$$F[\Delta_+, \Delta_-] = a(T - T_c^+) \Delta_+^2 + a(T - T_c^-) \Delta_-^2 + \frac{1}{2}(u_+ \Delta_+^4 + 2u_\pm \Delta_-^2 \Delta_+^2 + u_- \Delta_-^4) \quad (\text{A1})$$

Using a change of the variable  $T_c^\pm = T_0 \pm g$ . In the co-existence regime, where both  $\Delta_+$  and  $\Delta_-$  are finite, minimization of the free energy leads to the following two equations

$$\begin{aligned} (a(T - T_0 - g) + u_+ \Delta_+^2 + u_\pm \Delta_-^2) &= 0 \\ (a(T - T_0 + g) + u_- \Delta_-^2 + u_\pm \Delta_+^2) &= 0 \end{aligned} \quad (\text{A2})$$

Solving (A2), we obtain

$$\Delta_+^2 = a \left( \frac{u_- - u_\pm}{u_+ u_- - u_\pm^2} \right) \left[ T_0 - T + \left( \frac{u_\pm + u_-}{u_- - u_\pm} \right) g \right] \quad (\text{A3})$$

$$\Delta_-^2 = a \left( \frac{u_+ - u_\pm}{u_+ u_- - u_\pm^2} \right) \left[ T_0 - T - \left( \frac{u_\pm + u_+}{u_+ - u_\pm} \right) g \right] \quad (\text{A4})$$

The condition  $\Delta_+ \rightarrow 0$  determines the phase boundary 1 into the  $\Delta_-$  phase on the left-hand side of the phase diagram below. Likewise, the condition  $\Delta_- \rightarrow 0$  determines the phase boundary into the  $\Delta_+$  phase on the right-hand side of the phase diagram. This then sets two phase boundaries

$$\begin{aligned} T_0 - T_{c2}^{(L)} + \left( \frac{u_\pm + u_-}{u_- - u_\pm} \right) g &= 0 \Rightarrow T_{c2}^{(L)} = T_0 + \left( \frac{u_\pm + u_-}{u_- - u_\pm} \right) g && \text{(Phase boundary 1)} \\ T_0 - T_{c2}^{(R)} - \left( \frac{u_\pm + u_+}{u_+ - u_\pm} \right) g &= 0 \Rightarrow T_{c2}^{(R)} = T_0 - \left( \frac{u_\pm + u_+}{u_+ - u_\pm} \right) g && \text{(Phase boundary 2)} \end{aligned} \quad (\text{A5})$$

As  $u_\pm$  is increased, the left-hand and right-hand second order phase boundaries converge into a single line, and for larger values of  $u_\pm$  the co-existence phase is replaced by a single first-order phase boundary. There are three scenarios, as illustrated in Fig. 1 below

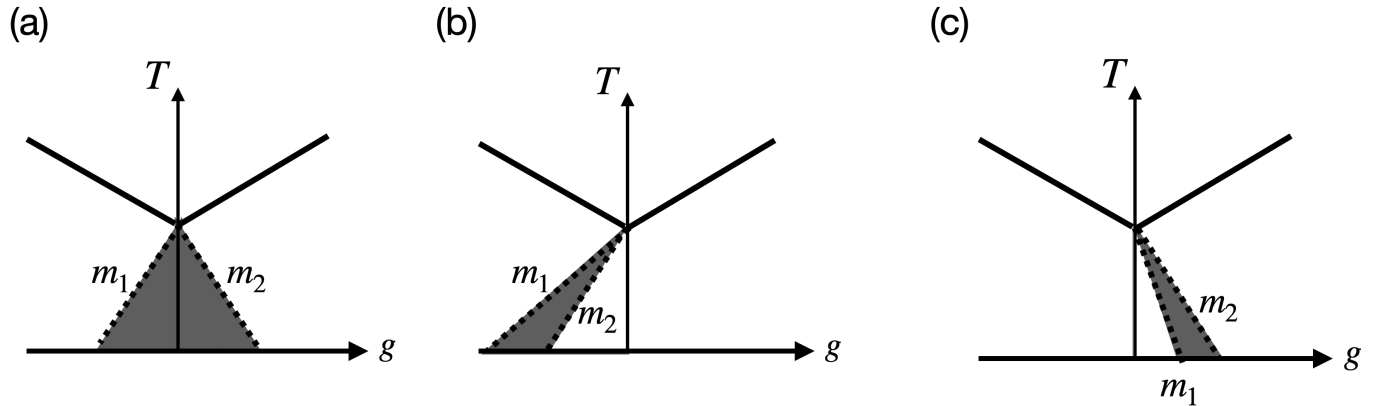


FIG. 1. Three possible scenarios for the parity-mixing region in  $g$ - $T$  space. (a)  $u_+ > u_- > u_\pm$ , (b)  $u_+ < u_\pm < u_-$  and (c)  $u_+ > u_\pm > u_-$

The two phase boundaries merge when the gradients become equal. If  $u_+ \neq u_-$ , then as  $u_\pm$  is increased, it must exceed  $\min(u_-, u_+)$ , leading to scenario (b) or (c), so that the criteria for the two phase boundaries to merge is then

$$m_1 = \left( \frac{u_\pm + u_-}{u_- - u_\pm} \right) = m_2 = - \left( \frac{u_\pm + u_+}{u_+ - u_\pm} \right). \quad (\text{A6})$$

which implies

$$u_{\pm}^2 = U_c^2 = u_+ u_- . \quad (\text{A7})$$

In the special case where  $u_+ = u_-$ , the criterion for merging of the two phases is the same. At the point of merger, when  $u_{\pm} = \sqrt{u_+ u_-}$ , the joint gradient of the phase boundary is then

$$m_1 = m_2 = m = \frac{dT_c}{dg} = \frac{\sqrt{u_+} + \sqrt{u_-}}{\sqrt{u_-} - \sqrt{u_+}} . \quad (\text{A8})$$

For larger values of  $u_{\pm} > U_c$ , the equilibrium values of the single order parameters are given by

$$\Delta_{\sigma} = \sqrt{\frac{a(T_c^{(\sigma)} - T)}{u_{\sigma}}}, \quad \Delta_{-\sigma} = 0, \quad \sigma = (-, +), \quad (\text{A9})$$

and the corresponding free energy is then given by

$$F_{\sigma} = -a^2 \left[ \frac{(T_0 - T + \sigma g)^2}{2u_{\sigma}} \right], \quad \sigma = (-, +). \quad (\text{A10})$$

The first order phase boundary separating the two phases occurs when  $F_+ = F_-$ , which then determines the phase boundary given by

$$\frac{(T_0 - T_c) + g}{\sqrt{u_+}} = \frac{(T_0 - T_c) - g}{\sqrt{u_-}}, \quad (\text{A11})$$

or

$$(T_c - T_0) = \left( \frac{\sqrt{u_+} + \sqrt{u_-}}{\sqrt{u_-} - \sqrt{u_+}} \right) g, \quad (\text{A12})$$

from which we see that the gradient  $m = dT_c/dg$  of the first order boundary matches the gradient found at the point of fusion between the two second-order phase boundaries (A8).